ACS OMEGA
http://pubs.acs.org/journal/acsodf
Article

Quantum Chemical Study of the Cycloaddition Reaction of Tropone with 1,1-Diethoxyethene Catalyzed by $B(C_6F_5)_3$ or BPh_3

Ken Sakata,* Sarina Suzuki, Tsubasa Sugimoto, and Takeshi Yoshikawa

Cite This: ACS Omega 2023, 8, 30410–30420
Read Online

ACCESS | Metrics & More | Article Recommendations | Supporting Information

ABSTRACT: Cycloaddition reaction of tropone with 1,1-diethoxyethene catalyzed by Lewis acid (LA), $B(C_6F_5)_3$ or BPh_3, was examined by using ωB97X-D-level density functional theory (DFT) calculations. In the absence of LA, the reaction proceeds in a stepwise fashion to form two chemical bonds, first between the C^2 atom in tropone and the C^2 atom in ethene and then between the C^5 atom in the former and the C^1 atom in the latter. When $B(C_6F_5)_3$ is attached to the O atom in tropone, the C^5 atom in tropone is attacked preferentially by the C^1 atom in ethene in the second stage. The attack of the O atom in tropone is shown to be less likely; thus, the [4 + 2] addition is favored in the $B(C_6F_5)_3$-catalyzed reaction. In contrast, the attack of the O atom in the BPh_3-attached tropone to the C^1 atom in ethene is preferred over the attack of the C^5 atom, indicating that the [8 + 2] cycloaddition instead of the [4 + 2] cycloaddition proceeds in the BPh_3-catalyzed reaction. Whether the C^1 atom in ethene is attacked by C^5 or by O in the second bond formation step is shown in this study to be governed mainly by the nucleophilicity of σ-lone pair electrons of the carbonyl O atom of tropone in the presence of LA. These results are consistent with the experiments reported by Li and Yamamoto.

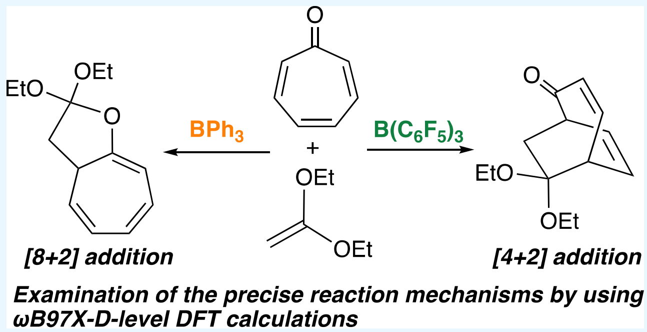

■ INTRODUCTION

Tropone and its derivatives have attracted the attention of both synthetic and theoretical chemists for more than half a century.[1−5] A variety of higher-order cycloaddition reactions utilizing its nonbenzenoid aromaticity, such as [6 + 3], [6 + 4], [8 + 2], and [8 + 3] additions, have been reported.[6−10] In contrast, the Diels−Alder [4 + 2] cycloaddition reaction is relatively limited because of the electron-deficient nature of tropones, although the reaction can directly provide the bicyclo[3.2.2] structures found in natural products or bioactive compounds.[11−16] Nozoe et al. examined the reaction of tropolones with maleic anhydride under reflux conditions and obtained [4 + 2] adducts.[11] Takeshita et al. reported the Diels−Alder reactions of tropones under high-pressure conditions.[12] Thus, harsh conditions are required for the Diels−Alder reaction of tropones.

One method for overcoming the low reactivity of tropones toward the [4 + 2] cycloaddition reaction is to increase the nucleophilicity for use as dienes in the normal-electron-demand Diels−Alder reactions. Jørgensen et al. reported Brønsted base-catalyzed asymmetric [4 + 2] cycloaddition reactions of tropolones.[17] Okamura et al. examined the Diels−Alder reaction between α-tropolone and electron-deficient dienophiles prompted by Et_3N or silica gel.[18] More recently, Wu et al. proposed a theoretical carbonyl umpolung strategy for activating tropone.[19]

Another method is the use of Lewis acid (LA) to activate tropones as dienes in the inverse-electron-demand Diels−Alder (IEDDA) reaction with electron-rich dienophiles. Li and Yamamoto reported the IEDDA reaction of tropone with electron-rich dienophiles.[20] Reaction of tropone (**1**) with 1,1-diethoxyethene (**2**) catalyzed by $B(C_6F_5)_3$ gave the [4 + 2] cycloadduct, 9,9-diethoxybicyclo[3.2.2]nona-3,6-dien-2-one (**3**), while the reaction catalyzed by other LAs such as BPh_3, Me_2AlCl, $BF_3{\cdot}OEt_2$, and $TiCl_4$ provided 2,2-diethoxy-3,3a-dihydro-2*H*-cyclohepta[*b*]furan (**4**), which corresponds to the [8 + 2] cycloadduct. Both **3** and **4** were obtained when Me_3Al, Et_2Zn, and $Ti(OiPr)_4$ were used as the LA catalyst. They further applied the bicyclo[3.2.2] compounds obtained by the $B(C_6F_5)_3$-catalyzed reaction to the formal synthesis of platencin.[21]

The difference in catalysis toward the IEDDA reaction among those LAs is of great interest to us. Domingo and Pérez recently examined the reactions of tropone with cyclic ketene acetal in the presence of $B(C_6F_5)_3$ or BF_3 by using molecular

Received: May 22, 2023
Accepted: July 27, 2023
Published: August 8, 2023

electron density theory, and concluded that a series of weak attractive/repulsive interactions control the selectivity in giving [4 + 2] or [8 + 2] cycloadduct.[22] In this study, we focused on the difference in catalytic roles for the cycloaddition reactions between $B(C_6F_5)_3$ and BPh_3, both of which have the same molecular structural frameworks, and examined the precise reaction mechanisms for the reaction of **1** with **2** catalyzed by $B(C_6F_5)_3$ or BPh_3, as shown in Scheme 1, by using *ω*B97X-D-level density functional theory (DFT) calculations.

Scheme 1. Reaction of 1 with 2 Catalyzed by a Lewis Acid (LA)

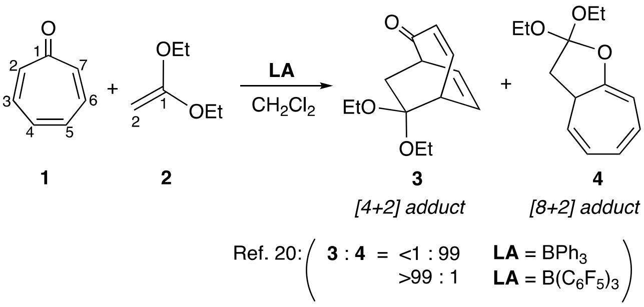

■ RESULTS AND DISCUSSION

Reaction without LA. We first examine the cycloaddition between **1** and **2** in the absence of LA. Stepwise pathways were found both for [4 + 2] and for [8 + 2] cycloadditions (Figure 1).[23] In the [4 + 2] addition pathway, nucleophilic attack of the C^2 atom in **2** by the C^2 atom in **1** gives an intermediate complex $\mathbf{INT_{A4}}$ through the transition state $\mathbf{TS1_{A4}}$. In $\mathbf{INT_{A4}}$, the distances between C^2 in **1** and C^2 in **2** and between C^5 in **1** and C^1 in **2** are 1.59 and 3.38 Å, respectively (Figure S2). The stability analysis for the solution of the closed-shell Kohn–Sham equations showed that the obtained Kohn–Sham wave function of $\mathbf{INT_{A4}}$ is stable. The bond formation between C^5 in **1** and C^1 in **2** proceeds through the second transition state $\mathbf{TS2_{A4}}$ to afford the [4 + 2] adduct **3**. The Gibbs free energies of $\mathbf{TS1_{A4}}$, $\mathbf{INT_{A4}}$, and $\mathbf{TS2_{A4}}$, relative to the initial state (**1** + **2**), ΔG^{298K}, are located relatively high, at 25.1, 18.9, and 22.1 kcal/mol, respectively (the activation energies, $\Delta G^{298K\ddagger}$, of $\mathbf{TS1_{A4}}$ and $\mathbf{TS2_{A4}}$ are 21.3 and 3.2 kcal/mol, respectively[24]). On the other hand, the transition state $\mathbf{TS1_{A8}}$, in which the direction of the C═C bond in dienophile is different from that in $\mathbf{TS1_{A4}}$, leads to the intermediate complex $\mathbf{INT_{A8}}$. The complex $\mathbf{INT_{A8}}$ provides the [8 + 2] product **4** through the transition state for the second bond formation between the O atom in **1** and the C^1 atom in **2**, $\mathbf{TS2_{A8}}$. The ΔG^{298K} of $\mathbf{TS1_{A8}}$, 27.5 kcal/mol ($\Delta G^{298K\ddagger}$ = 22.9 kcal/mol), is higher than that of $\mathbf{TS1_{A4}}$, while the ΔG^{298K} of $\mathbf{TS2_{A8}}$, 20.3 kcal/mol ($\Delta G^{298K\ddagger}$ = 1.1 kcal/mol), is slightly lower than that of $\mathbf{TS2_{A4}}$ (ΔG^{298K} = 22.1 kcal/mol; $\Delta G^{298K\ddagger}$ = 3.2 kcal/mol). In addition, the calculation revealed that the intermediate complex in the [4 + 2] addition pathway, $\mathbf{INT_{A4}}$, is transformed into $\mathbf{INT_{A8}}$ in the [8 + 2] addition pathway via rotation around the bond formed first between the C^2 atom in **1** and the C^2 atom in **2** through another transition state, $\mathbf{TS3_{A4}}$. One notes that the relative free energy of $\mathbf{TS3_{A4}}$ is not high, 22.5 kcal/mol ($\Delta G^{298K\ddagger}$ = 3.4 kcal/mol), compared with those of other transition states.

Thus, the first bond formation through $\mathbf{TS1_{A4}}$ is preferred over $\mathbf{TS1_{A8}}$. The resulting $\mathbf{INT_{A4}}$ leads, however, to $\mathbf{TS2_{A4}}$ and also to $\mathbf{TS3_{A4}}$ because these transition state structures have almost the same relative free energies (22.1 and 22.5 kcal/mol). This indicates that both **3** and **4** are formed in the addition of **1** and **2** in the absence of a catalyst (Scheme 2 and Figure S3). Experimentally, Takeshita et al. examined the cycloaddition reaction of tropone with 1,1-diethoxyethane under thermal conditions and observed [8 + 2], [4 + 2], and [6 + 2] cycloadducts.[12c] We could locate the transition state structure for bond formation between the C^7 atom in **1** and the C^1 atom in **2** to afford the [6 + 2] adduct **5**, $\mathbf{TS4_{A4}}$ (Figure S2). The ΔG^{298K} of $\mathbf{TS4_{A4}}$, 25.1 kcal/mol, is seen, however, to be higher than those of $\mathbf{TS2_{A4}}$ and $\mathbf{TS3_{A4}}$ to give **3** and **4**, respectively. We also examined transition state structures with other conformations of diethoxy moieties for the first bond formation (Figure S4), and $\mathbf{TS1_{A4}}$ has the lowest free energy among the obtained structures. Moreover, similar stepwise pathways were obtained for $\mathbf{TS1_{B4}}$ and $\mathbf{TS1_{B8}}$ (Figure S5).

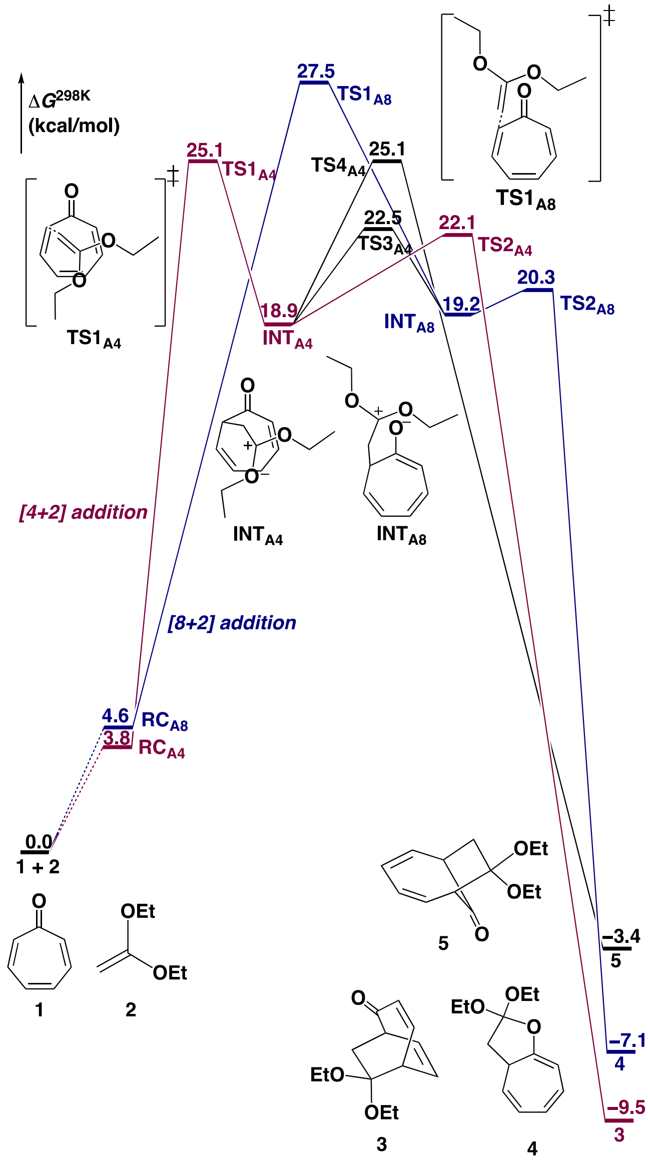

Figure 1. Gibbs free energy diagrams for the reaction of **1** with **2** without LA (kcal/mol). The [4 + 2] and [8 + 2] addition pathways are represented in red and blue, respectively.

$B(C_6F_5)_3$-Catalyzed Reaction. It was shown above to be difficult to obtain selectively the [4 + 2] or [8 + 2] cycloadduct in the reaction between **1** and **2** without any catalyst. The

https://doi.org/10.1021/acsomega.3c03560
ACS Omega 2023, 8, 30410−30420

Scheme 2. Pathways for the Reaction of 1 with 2 without LA

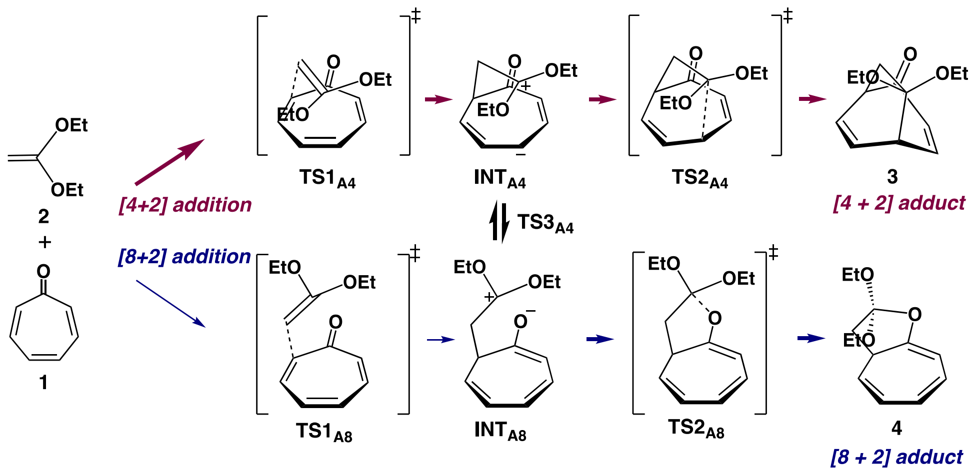

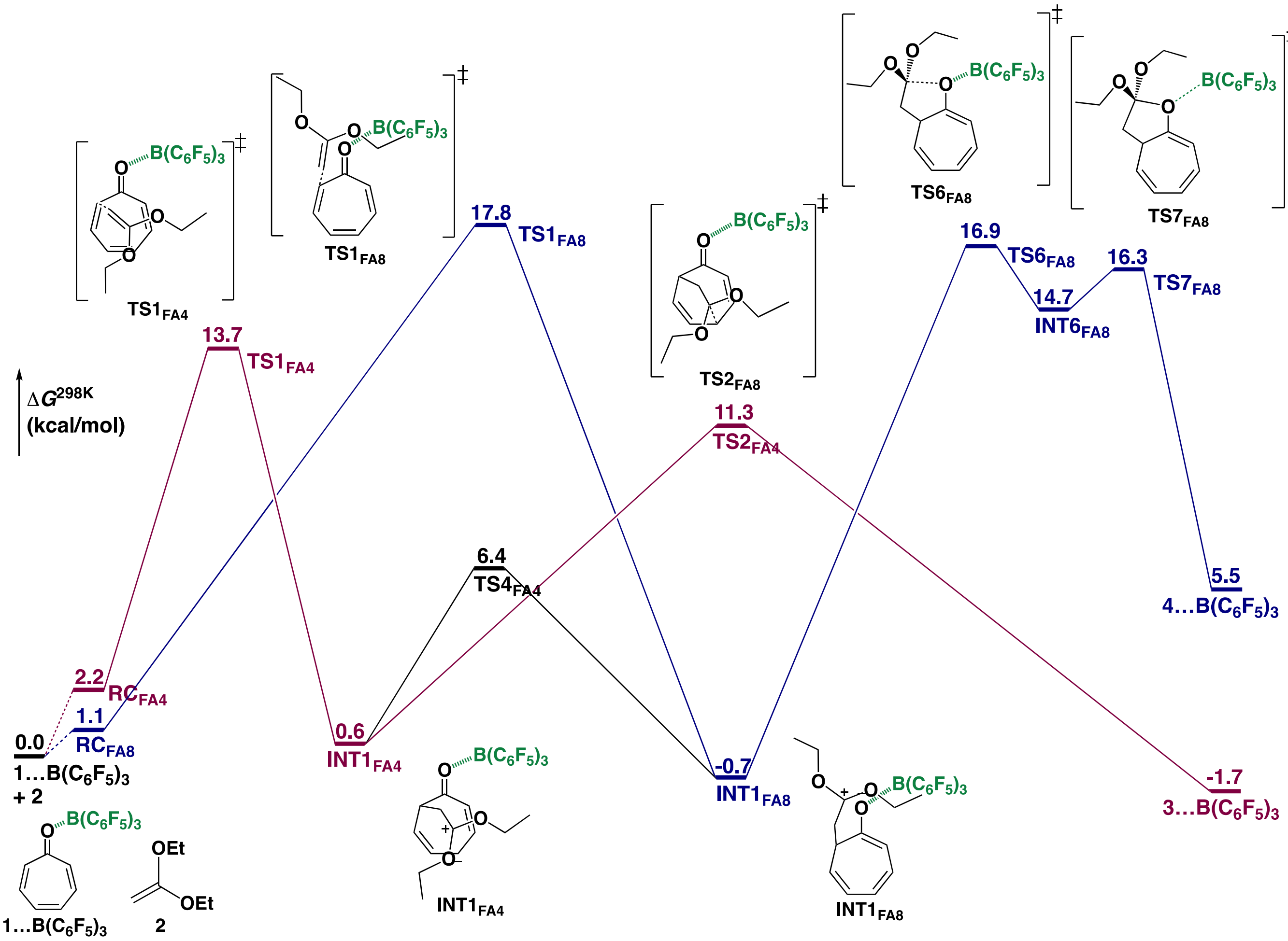

Figure 2. Gibbs free energy diagrams for the reaction of **1** with **2** catalyzed by $B(C_6F_5)_3$ (kcal/mol). The [4 + 2] and [8 + 2] addition pathways are represented in red and blue, respectively.

formation of two bonds should take place in a stepwise manner to avoid the strong overlap repulsion that would intervene in the cycloadditions.[25] We examine next the pathways for the reaction between tropone attached to $B(C_6F_5)_3$ (**1⋯B-(C_6F_5)$_3$**), which is lower in Gibbs free energy by 13.4 kcal/mol than (**1** + $B(C_6F_5)_3$), and **2**. As in the case of noncatalyzed reaction system, stepwise pathways were found both for the [4 + 2] and for the [8 + 2] cycloadditions (Figures 2 and S7). In the [4 + 2] addition pathway, the first bond formation through the transition state, **TS1$_{FA4}$**, is followed by the second bond formation through the intermediate complex **INT1$_{FA4}$** and the transition state **TS2$_{FA4}$** (Figure 3).[26] The ΔG^{298K} values of **TS1$_{FA4}$**, **INT1$_{FA4}$**, and **TS2$_{FA4}$**, are 13.7, 0.6, and 11.3 kcal/mol, respectively, much lower than those in the noncatalyzed reaction pathway ($\Delta G^{298K\ddagger}$ of **TS1$_{FA4}$** and **TS2$_{FA4}$** are 11.5 and 10.7 kcal/mol, respectively). In the [8 + 2] addition pathway,

https://doi.org/10.1021/acsomega.3c03560
ACS Omega 2023, 8, 30410−30420

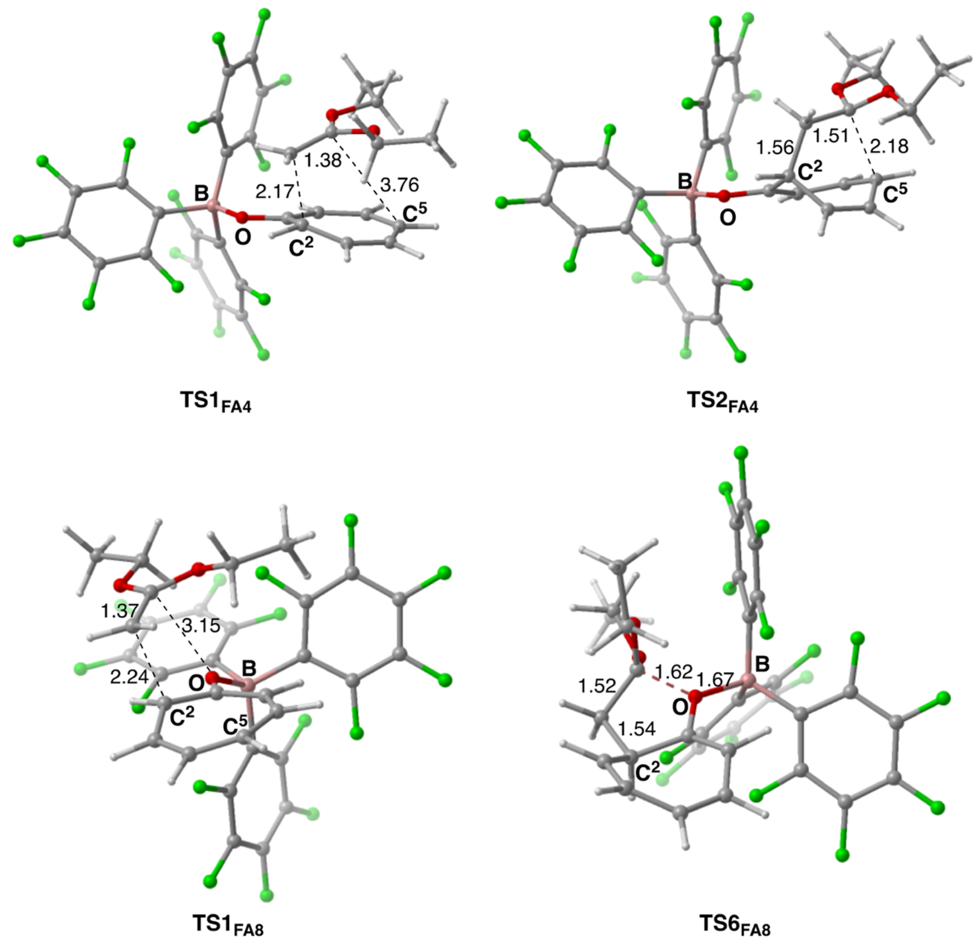

Figure 3. Structures of $\mathbf{TS1}_{\mathbf{FA4}}$, $\mathbf{TS2}_{\mathbf{FA4}}$, $\mathbf{TS1}_{\mathbf{FA8}}$, and $\mathbf{TS6}_{\mathbf{FA8}}$. Distances are shown in angstrom.

Scheme 3. Pathways for the Reaction of 1 with 2 Catalyzed by $B(C_6F_5)_3$

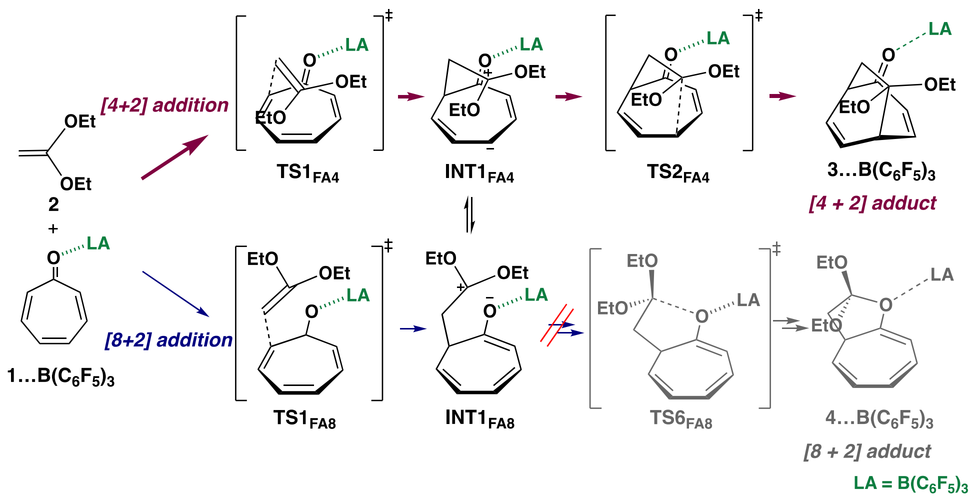

on the other hand, the first bond formation via the transition state $\mathbf{TS1}_{\mathbf{FA8}}$ (ΔG^{298K} = 17.8 kcal/mol; $\Delta G^{298K\ddagger}$ = 16.7 kcal/mol) gives an intermediate complex $\mathbf{INT1}_{\mathbf{FA8}}$ (ΔG^{298K} = −0.7 kcal/mol). This complex $\mathbf{INT1}_{\mathbf{FA8}}$, in which the dienophile moiety is located above the tropone plane, is then transformed into the other complex $\mathbf{INT2}_{\mathbf{FA8}}$ (ΔG^{298K} = 4.0 kcal/mol), in which the dienophile moiety lies on the side of tropone (Figures S7 and S8). The complex $\mathbf{INT2}_{\mathbf{FA8}}$ is further transformed into the other conformation complex $\mathbf{INT5}_{\mathbf{FA8}}$ ($\mathbf{INT2}_{\mathbf{FA8}}$ → $\mathbf{TS3}_{\mathbf{FA8}}$ (ΔG^{298K} = 5.8 kcal/mol) → $\mathbf{INT3}_{\mathbf{FA8}}$ (ΔG^{298K} = 2.2 kcal/mol) → $\mathbf{TS4}_{\mathbf{FA8}}$ (ΔG^{298K} = 6.3 kcal/mol) → $\mathbf{INT4}_{\mathbf{FA8}}$ (ΔG^{298K} = 4.7 kcal/mol) → $\mathbf{TS5}_{\mathbf{FA8}}$ (ΔG^{298K} = 6.0 kcal/mol) → $\mathbf{INT5}_{\mathbf{FA8}}$ (ΔG^{298K} = 5.5 kcal/mol; Figures S7 and S8)), and then the complex $\mathbf{INT5}_{\mathbf{FA8}}$ provides $\mathbf{INT6}_{\mathbf{FA8}}$ via the transition state, $\mathbf{TS6}_{\mathbf{FA8}}$, for the bond formation between the O atom in tropone and the C^1 atom in ethene (Figure 3 for the structure of $\mathbf{TS6}_{\mathbf{FA8}}$). The LA, $B(C_6F_5)_3$, is now dissociated from the O atom in tropone through $\mathbf{TS7}_{\mathbf{FA8}}$ to give finally the

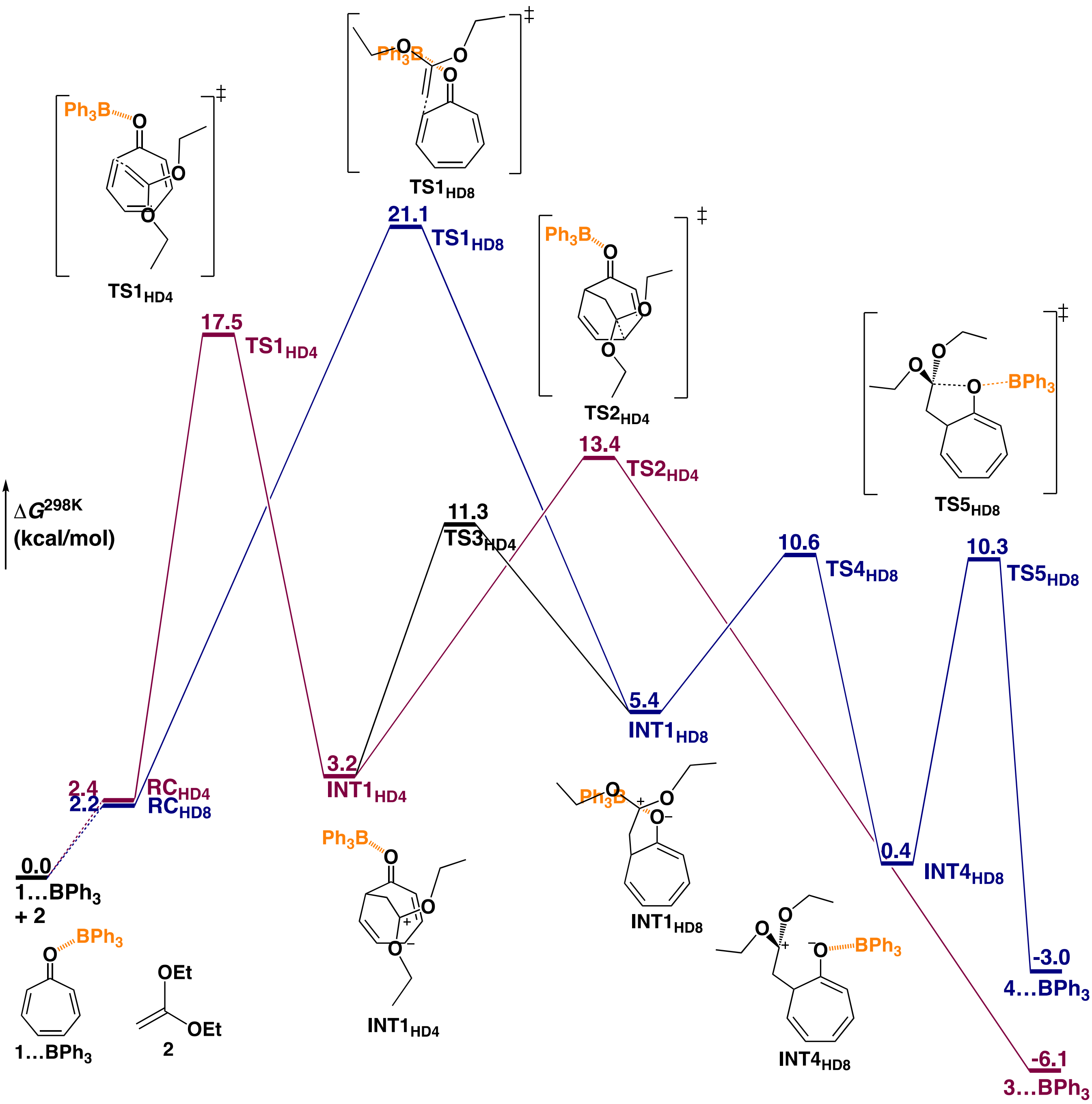

Figure 4. Gibbs free energy diagrams for the reaction of **1** with **2** catalyzed by BPh_3 (kcal/mol). The [4 + 2] and [8 + 2] addition pathways are represented in red and blue, respectively.

[8 + 2] cycloadduct **4···B(C$_6$F$_5$)$_3$** (Figure S8). The distance between the boron atom in $B(C_6F_5)_3$ and the oxygen atom in tropone at **INT5$_{FA8}$**, **TS6$_{FA8}$**, **INT6$_{FA8}$**, **TS7$_{FA8}$**, and **4···B(C$_6$F$_5$)$_3$** is 1.51, 1.67, 1.80, 1.89, and 4.18 Å, respectively. The ΔG^{298K} of **TS6$_{FA8}$** and **TS7$_{FA8}$** is 16.9 and 16.3 kcal/mol, much higher than that of **TS2$_{FA4}$** for the second bond formation in the [4 + 2] addition pathway ($\Delta G^{298K\ddagger}$ of **TS6$_{FA8}$** and **TS7$_{FA8}$** is 11.4 and 1.6 kcal/mol, respectively). The intermediate complex in the [4 + 2] addition pathway, **INT1$_{FA4}$**, is transformed into the intermediate complex in the [8 + 2] pathway, **INT1$_{FA8}$** (**INT1$_{FA4}$** (ΔG^{298K} = 0.6 kcal/mol) → **TS3$_{FA4}$** (ΔG^{298K} = 2.0 kcal/mol) → **INT2$_{FA4}$** (ΔG^{298K} = −0.4 kcal/mol) → **TS4$_{FA4}$** (ΔG^{298K} = 6.4 kcal/mol) → **INT3$_{FA4}$** (ΔG^{298K} = −0.5 kcal/mol) → **TS5$_{FA4}$** (ΔG^{298K} = 1.7 kcal/mol) → **INT4$_{FA4}$** (ΔG^{298K} = −1.0 kcal/mol) → **TS6$_{FA4}$** (ΔG^{298K} = 0.5 kcal/mol) → **INT5$_{FA4}$** (ΔG^{298K} = −0.7 kcal/mol) → **TS7$_{FA4}$** (ΔG^{298K} = 0.9 kcal/mol) → **INT1$_{FA8}$** (ΔG^{298K} = −0.7 kcal/mol); Figures 2, S7, and S8). One sees in Figure 2 shows that the [4 + 2] addition pathway should take place preferentially in the $B(C_6F_5)_3$-catalyzed reaction (Scheme 3).

BPh$_3$-Catalyzed Reaction. The stepwise pathways for the reaction between tropone attached to BPh_3 (**1···BPh$_3$**), which is lower in Gibbs free energy by 1.2 kcal/mol than (**1** + BPh_3), and **2** were examined next (Figures 4, 5, S9, and S10). For the [4 + 2] addition pathway, the first bond formation through the transition state, **TS1$_{HD4}$**, is followed by the second bond

https://doi.org/10.1021/acsomega.3c03560
ACS Omega 2023, 8, 30410−30420

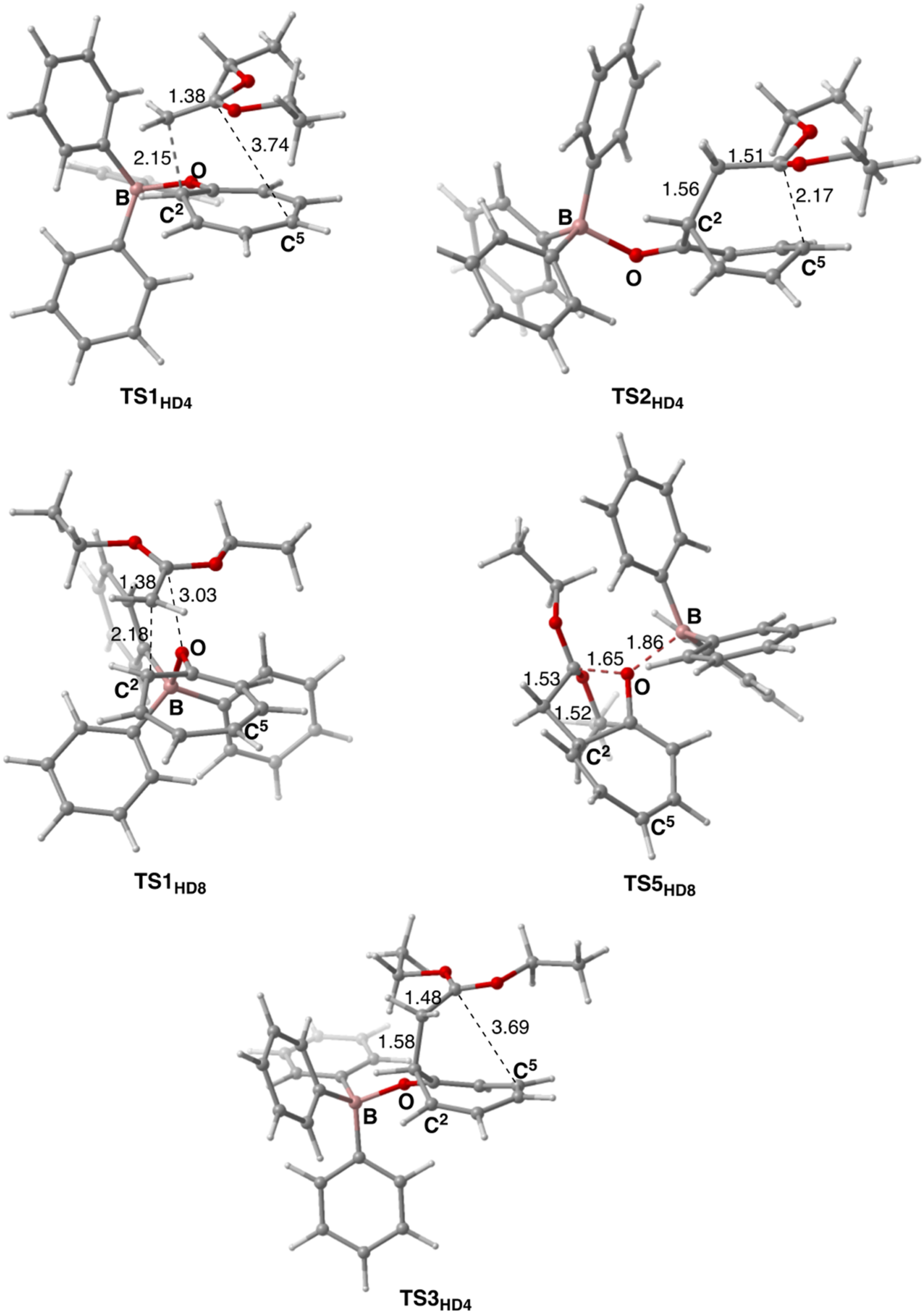

Figure 5. Structures of $\mathbf{TS1_{HD4}}$, $\mathbf{TS2_{HD4}}$, $\mathbf{TS1_{HD8}}$, $\mathbf{TS5_{HD8}}$, and $\mathbf{TS3_{HD4}}$. Distances are shown in angstrom.

formation through intermediate complex $\mathbf{INT1_{HD4}}$ and transition state $\mathbf{TS2_{HD4}}$ (Figure 5 for the structures of $\mathbf{TS1_{HD4}}$ and $\mathbf{TS2_{HD4}}$). The ΔG^{298K} of $\mathbf{TS1_{HD4}}$, $\mathbf{INT1_{HD4}}$, and $\mathbf{TS2_{HD4}}$ is 17.5, 3.2, and 13.4 kcal/mol, respectively, which are slightly higher than the corresponding values in the $B(C_6F_5)_3$-catalyzed pathway ($\Delta G^{298K\ddagger}$ of $\mathbf{TS1_{HD4}}$ and $\mathbf{TS2_{HD4}}$ is 15.1 and 10.2 kcal/mol, respectively).[27] In the [8 + 2] addition pathway, on the other hand, the ΔG^{298K} of the transition state for the first bond formation $\mathbf{TS1_{HD8}}$ and of the resulting intermediate complex $\mathbf{INT1_{HD8}}$ is 21.1 and 5.4 kcal/mol, respectively, being higher than those of $\mathbf{TS1_{HD4}}$ and $\mathbf{INT1_{HD4}}$ ($\Delta G^{298K\ddagger}$ of $\mathbf{TS1_{HD8}}$ is 18.9 kcal/mol). The migration of BPh_3 via $\mathbf{TS2_{HD8}}$ (ΔG^{298K} = 7.3 kcal/mol) and the rotation of a phenyl ring in BPh_3 via $\mathbf{TS3_{HD8}}$ (ΔG^{298K} = 6.5 kcal/mol) provide complex $\mathbf{INT3_{HD8}}$ (ΔG^{298K} = 5.1 kcal/mol; Figure S9). Further migration of both BPh_3 and the dienophile moiety gives complex $\mathbf{INT4_{HD8}}$ (ΔG^{298K} = 0.4 kcal/mol) via $\mathbf{TS4_{HD8}}$ (ΔG^{298K} = 10.6 kcal/mol). Finally, bond formation between the O atom in **1** and the C^1 atom in **2**, accompanied by a simultaneous bond breaking between the O atom in **1** and the B atom in BPh_3, gives the [8 + 2] cycloadduct $\mathbf{4{\cdots}BPh_3}$ via the transition state $\mathbf{TS5_{HD8}}$ (ΔG^{298K} = 10.3 kcal/mol and $\Delta G^{298K\ddagger}$ = 9.9 kcal/mol; Figure 5 for the structure of $\mathbf{TS5_{HD8}}$). The pathway from the complex $\mathbf{INT1_{HD8}}$ to $\mathbf{4{\cdots}BPh_3}$ is lower in free energy than $\mathbf{TS2_{HD4}}$ in the [4 + 2] pathway (ΔG^{298K} =

https://doi.org/10.1021/acsomega.3c03560
ACS Omega 2023, 8, 30410−30420

Scheme 4. Pathways for the Reaction of 1 with 2 Catalyzed by BPh_3

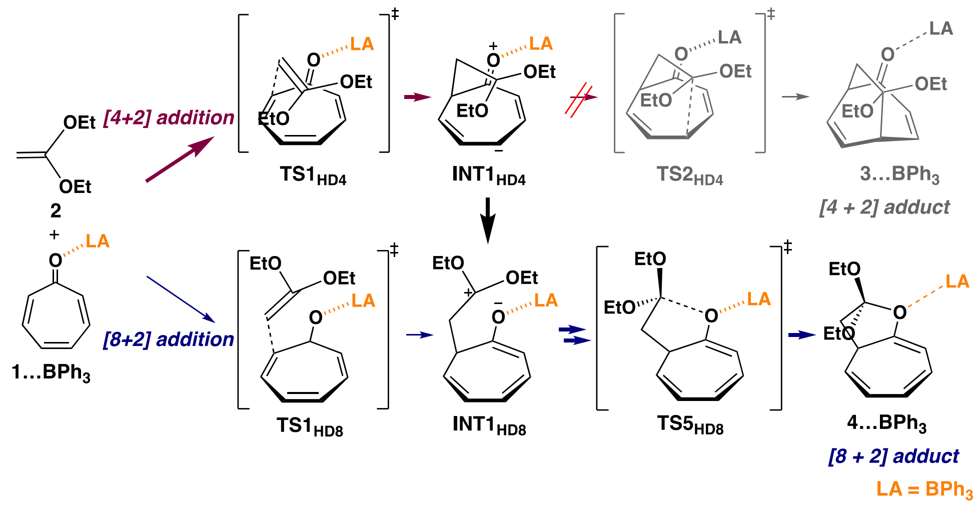

13.4 kcal/mol), although $\mathbf{TS1_{HD8}}$ in the [8 + 2] pathway is higher in free energy than $\mathbf{TS1_{HD4}}$ in the [4 + 2] pathway.

The intermediate complex in the [4 + 2] addition pathway, $\mathbf{INT1_{HD4}}$, is transformed easily into the complex in the [8 + 2] pathway, $\mathbf{INT1_{HD8}}$, via $\mathbf{TS3_{HD4}}$ (Figure 5 for the structure of $\mathbf{TS3_{HD4}}$). The ΔG^{298K} of $\mathbf{TS3_{HD4}}$ is 11.3 kcal/mol, which is lower than that of $\mathbf{TS2_{HD4}}$ (ΔG^{298K} = 13.4 kcal/mol; Figure 4). These results indicate that the [8 + 2] cycloadduct is produced preferentially through the transformation of $\mathbf{INT1_{HD4}}$ to $\mathbf{INT1_{HD8}}$ via $\mathbf{TS3_{HD4}}$ (Scheme 4).

Reactivity and Selectivity. We investigated orbital interactions for the noncatalyzed [4 + 2] cycloaddition by using the interaction frontier orbitals (IFOs)[28,25] calculated at the ωB97X/6-311G**(6d)//ωB97X-D(IEFPCM)/6-311G**(5d) level of theory. Electron delocalization from ethene to tropone at $\mathbf{TS1_{A4}}$ is represented by a pair of orbitals (ϕ_1'; ψ_1') (Figure S11a). The orbital ϕ_1' consists of the unoccupied Kohn–Sham orbitals of the tropone fragment, showing a large amplitude on the C^2 atom. The orbital ψ_1' is the π bonding orbital localized on the C=C bond of ethene, given by a linear combination of the occupied Kohn–Sham orbitals of the ethene fragment. The orbitals ϕ_1' and ψ_1' are located at +0.07 and −7.88 eV in energy, respectively. Electron delocalization from tropone to ethene is governed by a pair of orbitals (ϕ_2'; ψ_2') (Figure S11a). The orbital ϕ_2' is localized at the pπ orbital at the C^2 atom, which is composed of the occupied canonical orbitals of tropone. The orbital ψ_2' is the π antibonding orbital localized on the C=C bond, given by a combination of the unoccupied orbitals of ethene. The orbitals ϕ_2' and ψ_2' are located at −9.65 and +7.89 eV, respectively. The energy gap between ϕ_2' and ψ_2' is much larger than that between ϕ_1' and ψ_1'. That is, electron delocalization from ethene to tropone, inverse-electron demand, is essential for the first bond formation step of the [4 + 2] cycloaddition.[29]

At $\mathbf{TS2_{A4}}$ for the transition state structure in the second bond formation step giving the [4 + 2] adduct, electron delocalization from ethene to tropone is represented by a pair of orbitals (ϕ_3'; ψ_3'), as illustrated in Figure S11b. The orbitals, ϕ_3' and ψ_3' are localized around the bond formed through $\mathbf{TS1_{A4}}$, showing that electron delocalization remains of importance in strengthening the first bond between the C^2 atom in tropone and the C^2 atom in ethene. A pair of orbitals (ϕ_4'; ψ_4'), which shows the electron delocalization from tropone to ethene, come to have large amplitudes in between the C^5 atom in tropone and the C^1 atom in ethene. The energy gap between ϕ_4' and ψ_4' has been reduced compared with that between ϕ_2' and ψ_2' at $\mathbf{TS1_{A4}}$ (the orbitals ϕ_4' and ψ_4' are located at −8.89 and +2.34 eV in energy, respectively). Thus, the latter electron delocalization plays an important role in the formation of a bond between the C^5 atom in tropone and the C^1 atom in ethene.

Based on the results for the noncatalyzed cycloaddition, we next examined the first bond formation step in the [4 + 2] addition pathway in the presence of an LA. At $\mathbf{TS1_{FA4}}$, two pairs of interacting orbitals similar in shape to those in $\mathbf{TS1_{A4}}$ were obtained (Figures S12 and S13), indicating that the reaction mechanism is essentially unchanged by the attachment of $B(C_6F_5)_3$. However, the electron-accepting orbital ϕ_1'' is lowered by 2.00 eV compared to the orbital ϕ_1' in $\mathbf{TS1_{A4}}$. The electron-accepting ability of the C^2 atom in tropone is seen to be strengthened significantly by the attachment of $B(C_6F_5)_3$.[30] Meanwhile, the electron-donating orbital ψ_1'' of ethene is slightly elevated by 0.23 eV in $\mathbf{TS1_{FA4}}$ relative to the orbital ψ_1' in $\mathbf{TS1_{A4}}$. In response to the enhancement of the acidic character of the C^2 atom, the energy gap between the electron-donating and electron-accepting levels is significantly reduced in $\mathbf{TS1_{FA4}}$, compared with that in $\mathbf{TS1_{A4}}$, to facilitate electron delocalization. The first role of the LA is the strengthening of electrophilicity of the C^2 atom, consistent with findings reported by Domingo and Pérez.[22] At $\mathbf{TS1_{HD4}}$, the energy level of the electron-accepting orbital in tropone ϕ_1'' (Figure S12) is 1.45 eV lower than the orbital ϕ_1' in $\mathbf{TS1_{A4}}$, but 0.55 eV higher than the orbital ϕ_1'' in $\mathbf{TS1_{FA4}}$. This signifies that the electron-accepting ability of the C^2 atom in the BPh_3-attached tropone is weaker than that in the $B(C_6F_5)_3$-attached tropone but is significantly stronger than that in tropone without any LA. This difference in the strength of the electron-accepting ability of C^2 is reasoned in terms of the decrease in electron population and polarization of charges induced by the LA on the tropone framework. The natural population atomic charge of C^2 and the sum of the atomic charge in tropone at $\mathbf{TS1_{HD4}}$ are shown to be −0.165 and −0.064, and −0.129 and −0.018 at $\mathbf{TS1_{FA4}}$.[31,32] They were −0.182 and −0.466, respectively, in the noncatalyzed case.

For the second bond formation step in the [4 + 2] addition pathway in the presence of the LA, electron delocalization

https://doi.org/10.1021/acsomega.3c03560
ACS Omega 2023, 8, 30410−30420

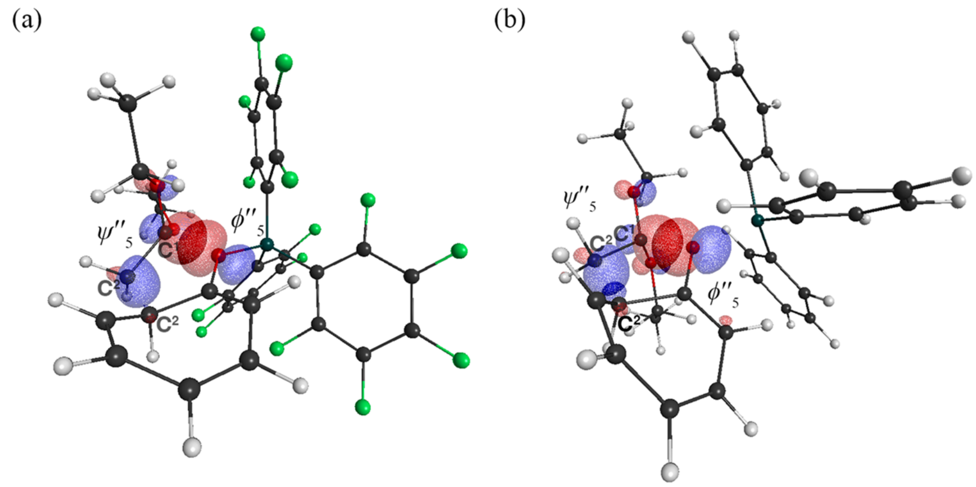

Figure 6. Pair of interacting orbitals (ϕ_5''; ψ_5'') for (a) $\mathbf{TS6_{FA8}}$ and (b) $\mathbf{TS5_{HD8}}$ calculated at the ωB97X-D/6-311G**(6d)//ωB97X-D(IEFPCM)/6-311G** level of theory. The orbitals ϕ_5'' for $\mathbf{TS6_{FA8}}$, ψ_5'' for $\mathbf{TS6_{FA8}}$, ϕ_5'' for $\mathbf{TS5_{HD8}}$, and ψ_5'' for $\mathbf{TS5_{HD8}}$ are located at −12.32, +2.05, −11.14, and +1.87 eV in energy, respectively.

from tropone to ethene is represented by a pair of orbitals, (ϕ_4''; ψ_4'') at $\mathbf{TS2_{FA4}}$ and $\mathbf{TS2_{HD4}}$ (Figure S14). The electron-donating orbitals, ϕ_4'' in $B(C_6F_5)_3$- and BPh_3-attached tropone, are −10.98 and −10.24 eV, respectively, showing that the nucleophilicity of the pπ-orbital in $B(C_6F_5)_3$-attached tropone is lower than that of BPh_3-attached tropone.

Next, we examine the orbital interactions at the transition state, $\mathbf{TS6_{FA8}}$ or $\mathbf{TS5_{HD8}}$, for bond formation between the O atom in $B(C_6F_5)_3$- or BPh_3-attached tropone and the C^1 atom in ethene in the [8 + 2] addition pathway. Electron delocalization from tropone to ethene at $\mathbf{TS6_{FA8}}$ is represented by a pair of orbitals (ϕ_5''; ψ_5''), as illustrated in Figure 6a. The electron-donating orbital ϕ_5'' is localized in the σ-lone pair orbital at the O atom, while the electron-accepting orbital ψ_5'' is the π-antibonding orbital localized on the C═C bond in ethene. At $\mathbf{TS5_{HD8}}$, a pair of orbitals very similar in shape was obtained (Figure 6b). The energy of the electron-donating orbital ϕ_5'', −11.14 eV, is higher than that in the $B(C_6F_5)_3$ attached tropone, −12.32 eV, indicating that the electron-donating ability of the σ-lone pair electrons at the O atom is considerably stronger in the BPh_3-attached tropone.

In summary, the attachment of the LA, $B(C_6F_5)_3$ or BPh_3, to tropone strengthens the electrophilicity of the pπ-orbital, having a large amplitude on the C^2 atom in tropone. The electrophilicity of the C^2 atom in the $B(C_6F_5)_3$-attached tropone is seen to be higher, as is expected from the stronger Lewis acidity of $B(C_6F_5)_3$ than that of BPh_3.[33,34] Thus, the first bond formation between the C^2 atom in the $B(C_6F_5)_3$-attached tropone and the C^2 atom in ethene is much easier in this step. In contrast, the LA weakens the electron-donating character of both the pπ-orbital in the tropone ring and the also σ-lone pair orbital on the O atom in tropone. In particular, the nucleophilicity of the σ-lone pair electrons on the O atom, which plays the dominant role in the second bond formation in the [8 + 2] cycloaddition, is weakened markedly by the attachment of the LA. Here, the effect of LA is seen to be more significant in the $B(C_6F_5)_3$-attached tropone.[35] Thus, the [8 + 2] addition is suppressed and the [4 + 2] addition proceeds in the case of $B(C_6F_5)_3$, whereas the [8 + 2] addition is preferred in the case of BPh_3.

■ CONCLUSIONS

We examined the cycloaddition reaction of tropone with 1,1-diethoxyethene catalyzed by an LA, $B(C_6F_5)_3$ or BPh_3, by using ωB97X-D-level DFT calculations. In the absence of a LA, we identified two stepwise pathways, the [4 + 2] and [8 + 2] additions. The first bond formation between C^2 in tropone and C^2 in 1,1-diethoxyethene prefers the [4 + 2] pathway, but the bond formation in the second stage between the C^5/O in tropone and C^1 in the ethene prefers the [8 + 2] process. In addition, the calculations revealed a path to transfer from the [4 + 2] pathway to the [8 + 2] pathway. Thus, both the [4 + 2] and [8 + 2] adducts were formed under a thermal condition. The LA-catalyzed additions take place in two stages, as is the case in the noncatalyzed cycloadditions. In the $B(C_6F_5)_3$-catalyzed reaction, the attack of the C^1 atom in ethene by the C^5 atom in tropone is preferred to the attack by the O atom in tropone in the second stage. On the contrary, the attack of the C^1 atom in ethene by the O atom in tropone is preferred in the BPh_3-catalyzed reaction, indicating that the formation of the [8 + 2] adduct is favored in this case. Whether C^1 of the dienophile is attacked by C^5 or by O of tropone in the second bond formation step is related to the nucleophilicity of the σ-lone pair electrons at the LA-attached O atom in tropone. These results are consistent with the experimental results reported by Li and Yamamoto.

■ COMPUTATIONAL DETAILS

DFT calculations were carried out with the Gaussian09[36] program package. Geometry optimization and analytical vibrational frequency analysis were performed by the restricted Kohn−Sham DFT by using the long-range corrected hybrid functionals with dispersion corrections (ωB97X-D).[37,38] A larger grid (superfinegrid) was used in the numerical integration.[36] Pople's 6-311G** basis set was used for the Gaussian basis functions (5d polarization functions).[39] The polarizable continuum model with integral equation formalism (IEFPCM)[40] was used for the solvent effects of dichloromethane. To confirm that the obtained transition state structures connect the reactant and product structures, IRC calculations[41] or structural optimizations from the initial structures which were displaced along the imaginary frequency

https://doi.org/10.1021/acsomega.3c03560
ACS Omega 2023, 8, 30410−30420

mode of the transition states were performed. To explore the conformers of **2**, the conformer search program CONFLEX[42] was initially used and the structures with lower energies were then optimized by using DFT calculations.

■ ASSOCIATED CONTENT

Supporting Information

The Supporting Information is available free of charge at https://pubs.acs.org/doi/10.1021/acsomega.3c03560.

Tables listing energies and geometries and figures containing optimized structures (PDF)

■ AUTHOR INFORMATION

Corresponding Author

Ken Sakata − *Faculty of Pharmaceutical Sciences, Toho University, Funabashi, Chiba 274-8510, Japan;* orcid.org/0000-0002-6920-0735; Email: ken.sakata@phar.toho-u.ac.jp

Authors

Sarina Suzuki − *Faculty of Pharmaceutical Sciences, Toho University, Funabashi, Chiba 274-8510, Japan*

Tsubasa Sugimoto − *Faculty of Pharmaceutical Sciences, Toho University, Funabashi, Chiba 274-8510, Japan*

Takeshi Yoshikawa − *Faculty of Pharmaceutical Sciences, Toho University, Funabashi, Chiba 274-8510, Japan;* orcid.org/0000-0002-7489-5252

Complete contact information is available at: https://pubs.acs.org/10.1021/acsomega.3c03560

Notes

The authors declare no competing financial interest.

■ ACKNOWLEDGMENTS

K.S. thanks Emeritus Professor Hiroshi Fujimoto of Kyoto University for his valuable discussion and comments. This work was supported by the JSPS KAKENHI, Grant Numbers 20K05532, 20H02733, and 20H05671, Japan. Some of the calculations were performed using the Research Center for Computational Science, Okazaki, Japan (Project: 23-IMS-C047). T.Y. and K.S. are grateful to the Center for generous permission to use its computing facilities.

■ REFERENCES

(1) (a) Pauson, P. L. Tropones and Tropolones. *Chem. Rev.* **1955**, *55*, 9−136. (b) Nozoe, T. Recent Advances in the Chemistry of Troponoids and Related Compounds in Japan. *Pure Appl. Chem.* **1971**, *28*, 239−280. (c) Pietra, F. Seven-Membered Conjugated Carbo- and Heterocyclic Compounds and their Homoconjugated Analogs and Metal Complexes. Synthesis, Biosynthesis, Structure, and Reactivity. *Chem. Rev.* **1973**, *73*, 293−364. (d) Pietra, F. Revival of Troponoid Chemistry. *Acc. Chem. Res.* **1979**, *12*, 132−138.

(2) Palazzo, T. A.; Mose, R.; Jørgensen, K. A. Cycloaddition Reactions: Why Is It So Challenging to Move from Six to Ten Electrons? *Angew. Chem., Int. Ed.* **2017**, *56*, 10033−10038.

(3) Frankowski, S.; Romaniszyn, M.; Skrzyńska, A.; Albrecht, Ł. The Game of Electrons: Organocatalytic Higher-Order Cycloadditions Involving Fulvene- and Tropone-Derived Systems. *Chem.—Eur. J.* **2020**, *26*, 2120−2132.

(4) Yu, P.; Chen, T. Q.; Yang, Z.; He, C. Q.; Patel, A.; Lam, Y.; Liu, C.-Y.; Houk, K. N. Mechanisms and Origins of Periselectivity of the Ambimodal [6 + 4] Cycloadditions of Tropone to Dimethylfulvene. *J. Am. Chem. Soc.* **2017**, *139*, 8251−8258.

(5) Chen, X.; Thøgersen, M. K.; Yang, L.; Lauridsen, R. F.; Xue, X.-S.; Jørgensen, K. A.; Houk, K. N. [8 + 2] vs [4 + 2] Cycloadditions of Cyclohexadienamines to Tropone and Heptafulvenes-Mechanisms and Selectivities. *J. Am. Chem. Soc.* **2021**, *143*, 934−944.

(6) Jessen, N. I.; McLeod, D.; Jørgensen, K. A. Higher-Order Cycloadditions in the Age of Catalysis. *Chem* **2022**, *8*, 20−30.

(7) For the [6 + 3] cycloadditions, see: (a) Trost, B. M.; Seoane, P. R. [6 + 3] Cycloaddition to Nine-membered Ring Carbocycles. *J. Am. Chem. Soc.* **1987**, *109*, 615−617. (b) Du, Y.; Feng, J.; Lu, X. A Phosphine-Catalyzed [3 + 6] Annulation Reaction of Modified Allylic Compounds and Tropone. *Org. Lett.* **2005**, *7*, 1987−1989. (c) Trost, B. M.; McDougall, P. J.; Hartmann, O.; Wathen, P. T. Asymmetric Synthesis of Bicyclo[4.3.1]decadienes and Bicyclo[3.3.2]decadienes via [6 + 3] Trimethylenemethane Cycloaddition with Tropones. *J. Am. Chem. Soc.* **2008**, *130*, 14960−14961. (d) Trost, B. M.; McDougall, P. J. Access to a Welwitindolinone Core Using Sequential Cycloadditions. *Org. Lett.* **2009**, *11*, 3782−3785. (e) Teng, H.-L.; Yao, L.; Wang, C.-J. Cu(I)-Catalyzed Regio- and Stereoselective [6 + 3] Cycloaddition of Azomethine Ylides with Tropone: An Efficient Asymmetric Access to Bridged Azabicyclo[4.3.1]decadienes. *J. Am. Chem. Soc.* **2014**, *136*, 4075−4080. (f) Liu, H.; Wu, Y.; Zhao, Y.; Li, Z.; Zhang, L.; Yang, W.; Jiang, H.; Chengfeng Jing, J.; Yu, H.; Wang, B.; Xiao, Y.; Guo, H. Metal-Catalyzed [6 + 3] Cycloaddition of Tropone with Azomethine Ylides: A Practical Access to Piperidine-Fused Bicyclic Heterocycles. *J. Am. Chem. Soc.* **2014**, *136*, 2625−2629. (g) Wu, Y.; Liu, H.; Zhang, L.; Sun, Z.; Xiao, Y.; Huang, J.; Wang, M.; Guo, H. Ag-Catalyzed Diastereoselective [6 + 3] Cycloaddition of Tropone with Homoserine Lactone-Derived Azomethine Ylides: Synthesis of Tricyclic Spiropiperidines. *RSC Adv.* **2016**, *6*, 73547−73550. (h) Guin, A.; Gaykar, R. N.; Deswal, S.; Biju, A. T. Three-Component, Diastereoselective [6 + 3] Annulation of Tropone, Imino Esters, and Arynes. *Org. Lett.* **2021**, *23*, 7456−7461.

(8) For the [6 + 4] cycloadditions, see: (a) Houk, K. N.; Luskus, L. J.; Bhacca, N. S. Novel Double [6 + 4] Cycloaddition of Tropone to Dimethylfulvene. *J. Am. Chem. Soc.* **1970**, *92*, 6392−6394. (b) Houk, K. N.; Watts, C. R. Cycloadditions of Tropone and Diphenylnitrileimine: A [6 + 4] 1,3-Dipolar Cycloaddition. *Tetrahedron Lett.* **1970**, *11*, 4025−4027. (c) Bonadeo, M.; De Micheli, C.; Gandolfi, R. Cycloadditions of Diphenylnitrilimine with Tropone and with Tricarbonyltroponeiron. Thermal [1,5] Sigmatropic Rearrangements of the [$_{\pi}6_s$+$_{\pi}4_s$] Cycloadducts of 1,3-Dipoles with Tropone. *J. Chem. Soc., Perkin Trans. 1* **1977**, 939−944. (d) Mukherjee, D.; Watts, C. R.; Houk, K. N. Periselectivity in the [4 + 2] and [6 + 4] Cycloadditions of Diphenylnitrilimine to Tropone. *J. Org. Chem.* **1978**, *43*, 817−821. (e) Rigby, J. H.; Ateeq, H. S.; Charles, N. R.; Cuisiat, S. V.; Ferguson, M. D.; Henshilwood, J. A.; Krueger, A. C.; Ogbu, C. O.; Short, K. M.; Heeg, M. J. Metal-promoted Higher-order Cycloaddition Reactions. Stereochemical, Regiochemical, and Mechanistic Aspects of the [6π + 4π] Reaction. *J. Am. Chem. Soc.* **1993**, *115*, 1382−1396. (f) Rigby, J. H.; Cuisiat, S. V. Synthetic Studies on the Ingenane Diterpenes. Construction of a Tetracyclic 8-Isoingenane Model. *J. Org. Chem.* **1993**, *58*, 6286−6291. (g) Isakovic, L.; Ashenhurst, J. A.; Gleason, J. L. Application of Lewis Acid Catalyzed Tropone [6 + 4] Cycloadditions to the Synthesis of the Core of CP-225,917. *Org. Lett.* **2001**, *3*, 4189−4192. (h) Rigby, J. H.; Fleming, M. Construction of the Ingenane Core Using an Fe(III) or Ti(IV) Lewis Acid Ccatalyzed Intramolecular [6 + 4] Cycloaddition. *Tetrahedron Lett.* **2002**, *43*, 8643−8646. (i) Rigby, J. H.; Chouraqui, G. First Intramolecular [6 + 4] Cycloaddition of Tropone and a Furan Moiety: Rapid Entry into a Highly Functionalized Ingenane Skeleton. *Synlett* **2005**, 2501−2503. (j) Ashenhurst, J. A.; Isakovic, L.; Gleason, J. L. Application of a [6 + 4] Cycloaddition Strategy Toward the Total Synthesis of CP-225,917. *Tetrahedron* **2010**, *66*, 368−378.

(9) For the [8 + 2] cycloadditions, see: (a) Kumar, K.; Kapur, A.; Ishar, M. P. S. Unusual [8 + 2] Annelation in the Reactions of Allenic Ester/Ketone-Derived 1,3-Dipoles with Tropone. *Org. Lett.* **2000**, *2*, 787−789. (b) Okamoto, J.; Yamabe, S.; Minato, T.; Hasegawa, T.; Machiguchi, T. Tropone Is a Mere Ketone for Cycloadditions to

Ketenes. *Helv. Chim. Acta* **2005**, *88*, 1519−1539. (c) Xie, M.; Liu, X.; Wu, X.; Cai, Y.; Lin, L.; Feng, X. Catalytic Asymmetric [8 + 2] Cycloaddition: Synthesis of Cycloheptatriene-Fused Pyrrole Derivatives. *Angew. Chem., Int. Ed.* **2013**, *52*, 5604−5607. (d) Wang, S.; Rodríguez-Escrich, C.; Fianchini, M.; Maseras, F.; Pericàs, M. A. Diastereodivergent Enantioselective [8 + 2] Annulation of Tropones and Enals Catalyzed by N-Heterocyclic Carbenes. *Org. Lett.* **2019**, *21*, 3187−3192. (e) He, C.; Li, Z.; Zhou, H.; Xu, J. Stereoselective [8 + 2] Cycloaddition Reaction of Azaheptafulvenes with *α*-Chloro Aldehydes via N-Heterocyclic Carbene Catalysis. *Org. Lett.* **2019**, *21*, 8022−8026.

(10) For the [8 + 3] cycloadditions, see: (a) Ishizu, T.; Masato Mori, M.; Kanematsu, K. High Periselectivity of 2-Oxyallyl Cations: Kinetic Evidence of the Cyclocoupling Reaction and Its Mechanistic Aspects. *J. Org. Chem.* **1981**, *46*, 526−531. (b) Nair, V.; Poonoth, M.; Vellalath, S.; Suresh, E.; Thirumalai, R. An N-Heterocyclic Carbene-Catalyzed [8 + 3] Annulation of Tropone and Enals via Homoenolate. *J. Org. Chem.* **2006**, *71*, 8964−8965. (c) Chen, C.; Shao, X.; Yao, K.; Yuan, J.; Shangguan, W.; Kawaguchi, T.; Shimazu, K. Unusual Catalytic Effect of the Two-Dimensional Molecular Space with Regular Triphenylphosphine Groups. *Langmuir* **2011**, *27*, 11958−11965. (d) Tejero, R.; Ponce, A.; Adrio, J.; Carretero, J. C. Ni-Catalyzed [8 + 3] Cycloaddition of Tropones with 1,1-Cyclopropanediesters. *Chem. Commun.* **2013**, *49*, 10406−10408. (e) Rivero, A. R.; Fernández, I.; Sierra, M. Á. Regio- and Diastereoselective Stepwise [8 + 3]-Cycloaddition Reaction between Tropone Derivatives and Donor−Acceptor Cyclopropanes. *Org. Lett.* **2013**, *15*, 4928−4931. (f) Liu, H.; Jia, H.; Shi, W.; Wang, C.; Zhang, C.; Guo, H. Nickel(II)-Catalyzed [8 + 3]-Cycloaddition of 2-Aryl-N-tosylaziridines with Tropone. *Org. Lett.* **2018**, *20*, 3570−3573. (g) McLeod, D. A.; Thøgersen, M. K.; Barløse, C. L.; Skipper, M. L.; Obregón, E. B.; Jørgensen, K. A. Enantioselective (8 + 3) Cycloadditions by Activation of Donor−Acceptor Cyclopropanes Employing Chiral Brønsted Base Catalysis. *Angew. Chem., Int. Ed.* **2022**, *61*, No. e202206096, DOI: 10.1002/anie.202206096.

(11) Nozoe, T.; Seto, S.; Ikemi, T. Diels-Alder Reaction of Tropolones with Maleic Anhydride. *Proc. Jpn. Acad.* **1951**, *27*, 655−657.

(12) (a) Tian, G. R.; Sugiyama, S.; Mori, A.; Takeshita, H. Novel Preparation of 1- and 3-Substituted Bicyclo[3.2.2]nona-3,6,8-trien-2-ones from Tropones and 2,3-Bis(methoxycarbonyl)-7-oxabicyclo[2.2.1] heptadiene by High-Pressure Cydoaddition-Thermal Cycloreversion Procedure. *Bull. Chem. Soc. Jpn.* **1988**, *61*, 2393−2399. (b) Takeshita, H.; Nakashima, H.; Sugiyama, S.; Mori, A. Novel Preparation of 1- and 3-Substituted Bicyclo[3.2.2]nona-3,6,8-trien-2-ones from Tropones and 2,3-Bis(methoxycarbonyl)-7-oxabicyclo[2.2.1]heptadiene by High-Pressure Cydoaddition-Thermal Cycloreversion Procedure. *Bull. Chem. Soc. Jpn.* **1988**, *61*, 573−574. (c) Mori, A.; Li, Z.-H.; Takeshita, H. High-Pressure Cycloaddition of Tropones to Ethoxyethene. An Occurrence of [4 + 2] and [8 + 2] Cycloadditions. *Bull. Chem. Soc. Jpn.* **1990**, *63*, 2257−2263.

(13) Cantrell, T. S. Reversal of Regiospecificity in Ground-State vs. Excited-State Cycloadditions. *Tetrahedron Lett.* **1975**, *16*, 907−908.

(14) (a) Rigby, J. H.; Sage, J. M.; Raggon, J. A Novel Entry into the Bicyclo[5.4.0]undecane Ring System. *J. Org. Chem.* **1982**, *47*, 4815−4816. (b) Rigby, J. H.; Sage, J. M. Short Synthesis of Bicyclo[3.2.2]-nona-3,6,8-trien-2-one. *J. Org. Chem.* **1983**, *48*, 3591−3592.

(15) Dahnke, K. R.; Paquette, L. A. Exploratory Synthetic Studies Involving the Tricyclo[9.3.0.0^{2,8}] tetradecane Ring System Peculiar to the Cyathins. *J. Org. Chem.* **1994**, *59*, 885−899.

(16) Thangaraj, B. M.; Bhojgude, S. S.; Bisht, R. H.; Gonnade, R. G.; Biju, A. T. Diels−Alder Reaction of Tropones with Arynes: Synthesis of Functionalized Benzobicyclo[3.2.2]nonatrienones. *J. Org. Chem.* **2014**, *79*, 4757−4762.

(17) Hammer, N.; Erickson, J. D.; Lauridsen, V. H.; Jakobsen, J. B.; Hansen, B. K.; Jacobsen, K. M.; Poulsen, T. B.; Jørgensen, K. A. Catalytic Asymmetric [4 + 2]-Cycloadditions Using Tropolones: Developments, Scope, Transformations, and Bioactivity. *Angew. Chem., Int. Ed.* **2018**, *57*, 13216−13220.

(18) Okamura, H.; Iiji, H.; Hamada, T.; Iwagawa, T.; Furuno, H. Diels−Alder Reaction of *α*-Tropolone and Electron-Deficient Dienophiles Prompted by Et_3N or Silica Gel: A New Synthetic Method of Highly Functionalized Homobarrelenone Derivatives. *Tetrahedron* **2009**, *65*, 10709−10714.

(19) Karas, L. J.; Campbell, A. T.; Alabugin, I. V.; Wu, J. I. Antiaromaticity Gain Activates Tropone and Nonbenzenoid Aromatics as Normal-Electron-Demand Diels−Alder Dienes. *Org. Lett.* **2020**, *22*, 7083−7087.

(20) Li, P.; Yamamoto, H. Lewis Acid Catalyzed Inverse-Electron-Demand Diels−Alder Reaction of Tropones. *J. Am. Chem. Soc.* **2009**, *131*, 16628−16629.

(21) Li, P.; Yamamoto, H. Formal Synthesis of Platencin. *Chem. Commun.* **2010**, *46*, 6294−6295.

(22) (a) Domingo, L. R.; Pérez, P. Understanding the Higher-Order Cycloaddition Reactions of Heptafulvene, Tropone, and Its Nitrogen Derivatives, with Electrophilic and Nucleophilic Ethylenes inside the Molecular Electron Density Theory. *New J. Chem.* **2022**, *46*, 11520−11530. (b) Domingo, L. R.; Pérez, P. A Molecular Electron Density Theory Study of the Higher-Order Cycloaddition Reactions of Tropone with Electron-Rich Ethylenes. The Role of the Lewis Acid Catalyst in the Mechanism and *Pseudocyclic* selectivity. *New J. Chem.* **2021**, *46*, 294−308. (c) Domingo, L. R.; Ríos-Gutiérrez, M.; Pérez, P. Unveiling the Chemistry of Higher-Order Cycloaddition Reactions within the Molecular Electron Density Theory. *Chemistry* **2022**, *4*, 735−752. (d) Domingo, L. R.; Ríos-Gutiérrez, M.; Pérez, P. Unveiling the Lewis Acid Catalyzed Diels−Alder Reactions Through the Molecular Electron Density Theory. *Molecules* **2020**, *25*, No. 2535, DOI: 10.3390/molecules25112535.

(23) We examined some other conformers for **2**. See Figure S1.

(24) The activation free energy of the transition state was estimated by the Gibbs free energy difference between the transition state and the immediately preceding intermediate complex.

(25) (a) Sakata, K.; Fujimoto, H. Quantum Chemical Study of Diels−Alder Reactions Catalyzed by Lewis Acid Activated Oxazaborolidines. *J. Org. Chem.* **2013**, *78*, 3095−3103. (b) Sakata, K.; Fujimoto, H. Origin of the *endo* Selectivity in the Diels−Alder Reaction between Cyclopentadiene and Maleic Anhydride. *Eur. J. Org. Chem.* **2016**, *2016*, 4275−4278. (c) Sakata, K.; Fujimoto, H. Roles of Lewis Acid Catalysts in Diels−Alder Reactions between Cyclopentadiene and Methyl Acrylate. *ChemistryOpen* **2020**, *9*, 662−4666.

(26) Some other transition state structures for the bond formation between the C^2 atom in **1** and the C^2 atom in **2** were calculated ($\mathbf{TS_{FB4}}$, $\mathbf{TS_{FC4}}$, and $\mathbf{TS_{FD4}}$ for the [4 + 2] addition and $\mathbf{TS_{FB8}}$, $\mathbf{TS_{FC8}}$, and $\mathbf{TS_{FD8}}$ for the [8 + 2] addition). See Figure S6.

(27) Some other transition state structures for the bond formation between the C^2 atom in 1 and the C^2 atom in 2 were calculated ($\mathbf{TS_{HA4}}$, $\mathbf{TS_{HB4}}$, and $\mathbf{TS_{HC4}}$ for the [4 + 2] addition and $\mathbf{TS_{HA8}}$, $\mathbf{TS_{HB8}}$, and $\mathbf{TS_{HC8}}$ for the [8 + 2] addition). See Figure S6.

(28) (a) Fukui, K.; Koga, N.; Fujimoto, H. Interaction Frontier Orbitals. *J. Am. Chem. Soc.* **1981**, *103*, 196−197. (b) Fujimoto, H. Paired Interacting Orbitals: A Way of Looking at Chemical Interactions. *Acc. Chem. Res.* **1987**, *20*, 448−453. (c) Sakata, K.; Fujimoto, H. Quantum Chemical Study of Lewis Acid Catalyzed Allylboration of Aldehydes. *J. Am. Chem. Soc.* **2008**, *130*, 12519−12526.

(29) Natural population analysis (ref 31) showed that the fragment charges at tropone and ethene are −0.424 and +0.424, respectively, at $\mathbf{TS1_{A4}}$. Thus, the global electron density transfer (GEDT) value, which has been proposed by Domingo, is 0.424e. For GEDT concept, see: Domingo, L. R. A New C−C Bond Formation Model Based on the Quantum Chemical Topology of Electron Density. *RSC Adv.* **2014**, *4*, 32415.

(30) The LUMO energy level of $\mathbf{1}\cdots\mathbf{B}(C_6F_5)_3$ is −2.19 eV, which is lower than that of **1** by 1.63 eV.

(31) For natural population analysis, see: Reed, A. E.; Curtiss, L. A.; Weinhold, F. Intermolecular Interactions from a Natural Bond Orbital, Donor-Acceptor Viewpoint. *Chem. Rev.* **1988**, *88*, 899−926.

(32) The sum of the atomic charges in $B(C_6F_5)_3$ at $\mathbf{TS1_{FA4}}$ and in BPh_3 at $\mathbf{TS1_{HD4}}$ are −0.408 and −0.366, respectively.
(33) The fluoride ion affinities of BPh_3 and $B(C_6F_5)_3$ have been estimated to be 320 and 448 kJ/mol, respectively. See Erdmann, P.; Leitner, J.; Schwarz, J.; Greb, L. An Extensive Set of Accurate Fluoride Ion Affinities for *p*-Block Element Lewis Acids and Basic Design Principles for Strong Fluoride Ion Acceptors. *ChemPhysChem* **2020**, *21*, 987−994.
(34) Sakata, K.; Fujimoto, H. Quantum Chemical Study of $B(C_6F_5)_3$-Catalyzed Hydrosilylation of Carbonyl Group. *J. Org. Chem.* **2013**, *78*, 12505−12512.
(35) The natural population charges of the O atom in $\mathbf{1{\cdots}B(C_6F_5)_3}$, and $\mathbf{1{\cdots}BPh_3}$ are −0.57 and −0.56, respectively, which are almost the same as the charge in **1**, −0.57. The attachment of the Lewis acid decreases the electronic population of the s and σ−p orbitals in the oxygen atom, while it prompts the polarization of π orbitals, increasing the π−p orbitals. The decrease in the population of the s and σ−p orbitals in the oxygen atom attached to $B(C_6F_5)_3$ is larger than that in the oxygen atom attached to BPh_3 (Figure S15).
(36) Frisch, M. J.; Trucks, G. W.; Schlegel, H. B.; Scuseria, G. E.; Robb, M. A.; Cheeseman, J. R.; Scalmani, G.; Barone, V.; Mennucci, B.; Petersson, G. A.; Nakatsuji, H.; Caricato, M.; Li, X.; Hratchian, H. P.; Izmaylov, A. F.; Bloino, J.; Zheng, G.; Sonnenberg, J. L.; Hada, M.; Ehara, M.; Toyota, K.; Fukuda, R.; Hasegawa, J.; Ishida, M.; Nakajima, T.; Honda, Y.; Kitao, O.; Nakai, H.; Vreven, T.; Montgomery, J. A., Jr.; Peralta, J. E.; Ogliaro, F.; Bearpark, M.; Heyd, J. J.; Brothers, E.; Kudin, K. N.; Staroverov, V. N.; Kobayashi, R.; Normand, J.; Raghavachari, K.; Rendell, A.; Burant, J. C.; Iyengar, S. S.; Tomasi, J.; Cossi, M.; Rega, N.; Millam, J. M.; Klene, M.; Knox, J. E.; Cross, J. B.; Bakken, V.; Adamo, C.; Jaramillo, J.; Gomperts, R.; Stratmann, R. E.; Yazyev, O.; Austin, A. J.; Cammi, R.; Pomelli, C.; Ochterski, J. W.; Martin, R. L.; Morokuma, K.; Zakrzewski, V. G.; Voth, G. A.; Salvador, P.; Dannenberg, J. J.; Dapprich, S.; Daniels, A. D.; Farkas, Ö.; Foresman, J. B.; Ortiz, J. V.; Cioslowski, J.; Fox, D. J. *Gaussian 09*, revision D.01; Gaussian, Inc.: Wallingford, CT, 2009.
(37) (a) Hohenberg, P.; Kohn, W. Inhomogeneous Electron Gas. *Phys. Rev.* **1964**, *136*, 864−871. (b) Kohn, W.; Sham, L. J. Self-Consistent Equations Including Exchange and Correlation Effects. *Phys. Rev.* **1965**, *140*, A1133−A1138.
(38) Chai, J.-D.; Head-Gordon, M. Long-Range Corrected Hybrid Density Functionals with Damped Atom−Atom Dispersion Corrections. *Phys. Chem. Chem. Phys.* **2008**, *10*, 6615−6620.
(39) Hehre, W. J.; Radom, L.; Schleyer, P. v. R.; Pople, J. A. *Ab Initio Molecular Orbital Theory*; Wiley: New York, 1986.
(40) (a) Miertuš, S.; Scrocco, E.; Tomasi, J. Electrostatic Interaction of a Solute with a Continuum. A Direct Utilizaion of Ab Initio Molecular Potentials for the Prevision of Solvent Effects. *Chem. Phys.* **1981**, *55*, 117−129. (b) Scalmani, G.; Frisch, M. Continuous Surface Charge Polarizable Continuum Models of Solvation. I. General Formalism. *J. Chem. Phys.* **2010**, *132*, No. 114110, DOI: 10.1063/1.3359469.
(41) Fukui, K. The path of chemical reactions - the IRC approach. *Acc. Chem. Res.* **1981**, *14*, 363−368.
(42) (a) Goto, H.; Osawa, E. Corner Flapping: A Simple and Fast Algorithm for Exhaustive Generation of Ring Conformations. *J. Am. Chem. Soc.* **1989**, *111*, 8950−8951. (b) Gotō, H.; Osawa, E. An Efficient Algorithm for Searching Low-Energy Conformers of Cyclic and Acyclic Molecules. *J. Chem. Soc., Perkin Trans. 2* **1993**, *2*, 187−198.

https://doi.org/10.1021/acsomega.3c03560
ACS Omega 2023, 8, 30410−30420